

# SENSITIVITY ANALYSIS OF WIND AND TEMPERATURE RETRIEVALS FROM COHERENT DOPPLER LIDAR DATA: Results from the first dual-Doppler validation study

ROB K NEWSOM<sup>1</sup>, DAVID LIGON<sup>2</sup>, RON CALHOUN<sup>3</sup>, EDWARD CREEGAN<sup>2</sup>, ROB HEAP<sup>3</sup>, MARKO PRINCEVAC<sup>3</sup>

<sup>1</sup>Cooperative Institute for Research in the Atmosphere, Colorado State University

<sup>2</sup>US Army Research Laboratory

<sup>3</sup>Environmental Fluid Dynamics Program, Arizona State University

## INTRODUCTION

The Joint Urban 2003 (JU2003) field experiment was conducted in Oklahoma City during the summer of 2003. The purpose of this experiment was to better understand dispersion of chemical and/or airborne biological contaminants in an urban environment. Numerous samplers and meteorological sensors were deployed in and around the central business district (CBD) of Oklahoma City. One very unique aspect of this experiment involved the deployment of two Doppler lidars at locations outside the CBD. The function of the lidars was to provide spatially and temporally resolved observations of the "urban-scale" flow. In this study, we use the dual-Doppler lidar dataset from JU2003 to test the output of an algorithm that retrieves micro-scale flow structures from single-Doppler lidar data using four-dimensional variational data assimilation (4DVAR). Retrievals of  $u$ ,  $v$ ,  $w$  and  $\theta$  are performed using data from one of the lidars. The radial component of the retrieved velocity field relative to the second lidar is then compared to the measured radial velocity field from the second lidar. This is the first time that such a comparison has been possible.

## EXPERIMENTAL SETUP

Two WindTracer<sup>®</sup> Doppler lidars were used in the JU2003 experiment. One system is owned by the US Army Research Laboratory (ARL) and the other system is owned by Arizona State University (ASU). The WindTracer<sup>®</sup> lidar, which is manufactured by CLR Photonics, employs a solid state laser transmitter operating at a wavelength of 2µm and a pulse repetition frequency of 500 Hz. The WindTracer<sup>®</sup> lidar measures range resolved profiles of radial velocity and aerosol backscatter.

The figure on the lower left shows a map of Oklahoma City and the locations of the ARL and ASU lidars. Also indicated are the areas covered by the scans (solid lines), and the model domain (dashed line). The ARL lidar was deployed approximately 1.5 km east-northeast of the CBD, and the ASU lidar was located approximately 3.8 km to the south and 1 km to the east of the ARL lidar. Data used in this study was acquired on 11 July, 2003 at about 1800 UTC (1300 CDT). The ARL lidar performed a series of RHI raster scans with elevation angles ranging from 0° to 45° at 8° intervals, and azimuth angles ranging from 184.4° to 244.4° in 5° steps. The ASU lidar performed a similar type scan with azimuth angles ranging from 275° to 335°. Signal processing for both systems was configured to give 66-m range resolution and 100 pulse averaging, implying a 5 Hz beam rate. The figure on the lower right is a graphical depiction of overlapping RHI scans. Colors represent the radial velocities measured relative to each lidar location. Retrievals were performed by defining a coordinate system with an origin centered on the location of the ARL lidar. The computational domain extended from -5 km to 0.5 km in  $x$  (east-west), -5 km to 0.5 km in  $y$  (north-south), and 0 km to 2.0 km in  $z$  (vertical).

## RETRIEVAL METHOD

The retrieval algorithm attempts to fit the output of a prognostic model to spatially and temporally resolved measurements of radial velocity. The fit is performed by variational adjustment of the model's initial state using the adjoint method. For this study, the model is given by a system of equations that simulate dry, shallow incompressible flow using the Boussinesq approximation. The model equations are given by

$$\frac{\partial u}{\partial t} + \frac{\partial u}{\partial x} u + \frac{\partial u}{\partial y} v + \frac{\partial u}{\partial z} w = -\frac{\partial \phi}{\partial x} + \nu \nabla^2 u$$

$$\frac{\partial v}{\partial t} + \frac{\partial v}{\partial x} u + \frac{\partial v}{\partial y} v + \frac{\partial v}{\partial z} w = -\frac{\partial \phi}{\partial y} + \nu \nabla^2 v$$

$$\frac{\partial w}{\partial t} + \frac{\partial w}{\partial x} u + \frac{\partial w}{\partial y} v + \frac{\partial w}{\partial z} w = -\frac{\partial \phi}{\partial z} + \nu \nabla^2 w$$

The acceleration of gravity is  $g$ ,  $\phi$  is a reference virtual potential temperature,  $p$  is the pressure normalized by a constant air density. Horizontally averaged variables are enclosed in brackets. The virtual potential temperature is  $\theta = \theta_0 + \theta'$  where  $\theta_0$  is the base-state virtual potential temperature and  $\theta'$  the departure from the base-state. The initial conditions are adjusted in order to minimize a penalized cost function. The primary term in the cost function is a measure of the error between the model output and the lidar measurements. This is given by

$$J_{\text{min}} = \sum_{i=1}^N \frac{(\Delta u_i)^2}{\sigma_i^2}$$

$$\Delta u_i = u_i - u_i^{\text{obs}}$$

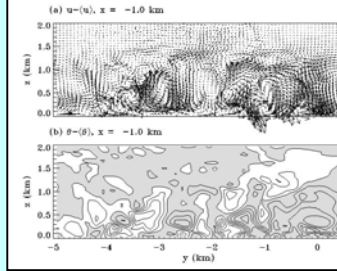
The summation in the above expression is performed over all radial velocity observations within the model domain and assimilation time. There are  $M$  individual radial velocity observations. The unit vector from the lidar to the  $m^{\text{th}}$  observation is  $\mathbf{r}_m$ . The observed radial velocity is  $u_m^{\text{obs}}$  and the corresponding error is  $\sigma_m$ . The velocity field generated by the model is denoted by  $\mathbf{u}_m$  where the overbar implies interpolation to the coordinates of the  $m^{\text{th}}$  observation. Estimates of the measurement precision were obtained from time series analysis of fixed beam data.

## OBSERVATIONS

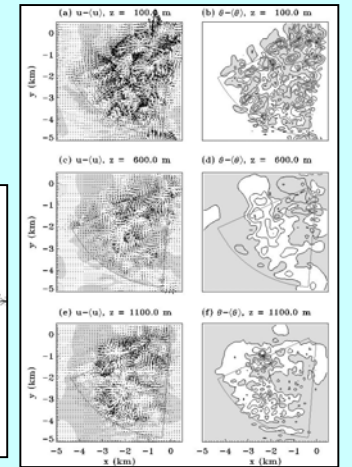
Single-Doppler retrievals of micro-scale wind and temperature fields were performed using data from the ARL WindTracer<sup>®</sup> lidar. The figure on the lower left shows individual RHI scans at the start and end of the assimilation period for both the ARL and ASU lidars. To clarify, the  $x$ -axis in these panels is actually the horizontal range from the respective lidars and should not be confused with the  $x$ -coordinate of the computational domain.

The figure on the lower right shows vertical profiles of the "base-state" wind and virtual potential fields. The velocity profiles were obtained from a VAD-type analysis of the ARL raster scan data. The virtual potential temperature profile was obtained from a radiosonde release near the CBD at approximately 1800 UTC (1300 CDT). Conditions at the time were hot and fairly humid, with clear skies and winds out of the south at 5 to 8  $\text{ms}^{-1}$  below 200 m AGL.

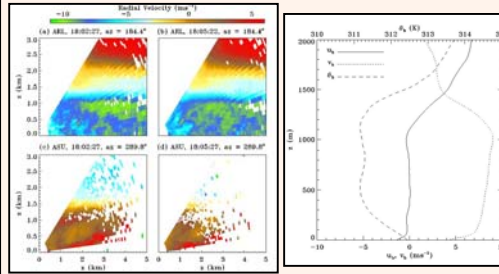
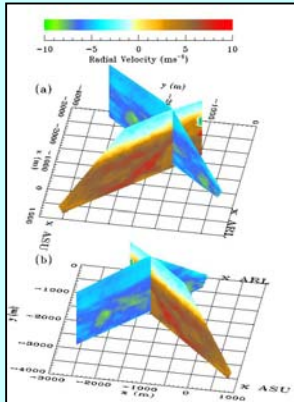
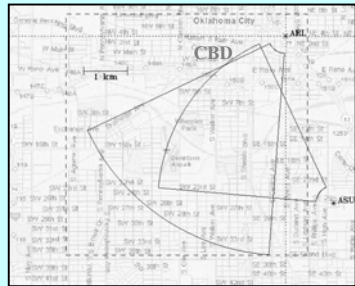
## RESULTS



The panels above show two-dimensional vertical cross sections of the retrieved perturbation  $u'-v'$  vector field (a) and contours of the perturbation virtual potential temperature field (b) from the middle of the assimilation period. Perturbation variables are obtained by subtracting the horizontal mean. In (b) the gray areas indicate negative values.



The panels above show two-dimensional horizontal cross sections of the retrieved perturbation  $u'-v'$  vector field (left panels) and contours of the perturbation virtual potential temperature field (right panels) from the middle of the assimilation period at three selected vertical levels. In (a), (c), and (e) the gray areas indicate regions of negative virtual velocity. In (b), (d) and (f) the gray areas indicate regions of negative perturbation virtual potential temperature.



To assess the accuracy and reliability of the single-Doppler retrieval the correlation and RMS deviations between the retrieved field and that observed by the ASU lidar were computed. The component of the wind vector field along the line-of-sight of the ASU lidar ( $\mathbf{u} \cdot \mathbf{r}_{ASU}$ ) was computed by linearly interpolating to the space and time coordinates of the ASU lidar measurements. That result was then compared directly to the radial velocity measurements from the ASU lidar ( $u_{ASU}$ ). The panels below show the result of this comparison. A correlation diagram between  $\mathbf{u} \cdot \mathbf{r}_{ASU}$  and  $u_{ASU}$  is shown in panel (a). A histogram of the percent occurrence of the difference  $\mathbf{u} \cdot \mathbf{r}_{ASU} - u_{ASU}$  is shown in panel (b). The linear correlation coefficient between  $\mathbf{u} \cdot \mathbf{r}_{ASU}$  and  $u_{ASU}$  was found to be 0.93. The RMS deviation between  $\mathbf{u} \cdot \mathbf{r}_{ASU}$  and  $u_{ASU}$  was found to be 1.4  $\text{m s}^{-1}$ .

